









RESEARCH ARTICLE | AUGUST 24 2022

Microfluidic synthesis as a new route to produce novel functional materials

Xinying Xie ; Yisu Wang; Sin-Yung Siu ; Chiu-Wing Chan ; Yujiao Zhu ; Xuming Zhang ; Jun Ge ; Kangning Ren  



Biomicrofluidics 16, 041301 (2022)

<https://doi.org/10.1063/5.0100206>



CrossMark



AIP Advances

Why Publish With Us?



25 DAYS
average time
to 1st decision



740+ DOWNLOADS
average per article



INCLUSIVE
scope

[Learn More](#)

 AIP
Publishing

Microfluidic synthesis as a new route to produce novel functional materials

Cite as: Biomechanics 16, 041301 (2022); doi: 10.1063/5.0100206

Submitted: 22 May 2022 · Accepted: 28 July 2022 ·

Published Online: 24 August 2022



Xinying Xie,¹ Yisu Wang,¹ Sin-Yung Siu,¹ Chiu-Wing Chan,¹ Yujiao Zhu,^{1,2} Xuming Zhang,² Jun Ge,^{3,4} and Kangning Ren^{1,5,6,a)}

AFFILIATIONS

¹Department of Chemistry, Hong Kong Baptist University, Hong Kong 999077, China

²Department of Applied Physics, Hong Kong Polytechnic University, Hong Kong 999077, China

³Key Laboratory for Industrial Biocatalysis, Ministry of Education, Department of Chemical Engineering, Tsinghua University, Beijing 100084, China

⁴Institute of Biopharmaceutical and Health Engineering, Tsinghua Shenzhen International Graduate School, Shenzhen 518055, China

⁵State Key Laboratory of Environmental and Biological Analysis, Hong Kong Baptist University, Hong Kong 999077, China

⁶HKBU Institute of Research and Continuing Education, Hong Kong Baptist University, Shenzhen 518057, China

^{a)}Author to whom correspondence should be addressed: kangningren@gmail.com and kangningren@hkbu.edu.hk

ABSTRACT

By geometrically constraining fluids into the sub-millimeter scale, microfluidics offers a physical environment largely different from the macroscopic world, as a result of the significantly enhanced surface effects. This environment is characterized by laminar flow and inertial particle behavior, short diffusion distance, and largely enhanced heat exchange. The recent two decades have witnessed the rapid advances of microfluidic technologies in various fields such as biotechnology; analytical science; and diagnostics; as well as physical, chemical, and biological research. On the other hand, one additional field is still emerging. With the advances in nanomaterial and soft matter research, there have been some reports of the advantages discovered during attempts to synthesize these materials on microfluidic chips. As the formation of nanomaterials and soft matters is sensitive to the environment where the building blocks are fed, the unique physical environment of microfluidics and the effectiveness in coupling with other force fields open up a lot of possibilities to form new products as compared to conventional bulk synthesis. This Perspective summarizes the recent progress in producing novel functional materials using microfluidics, such as generating particles with narrow and controlled size distribution, structured hybrid materials, and particles with new structures, completing reactions with a quicker rate and new reaction routes and enabling more effective and efficient control on reactions. Finally, the trend of future development in this field is also discussed.

Published under an exclusive license by AIP Publishing. <https://doi.org/10.1063/5.0100206>

INTRODUCTION

In some ways, the applications of microfluidic technologies could be dated back to the debut of some broadly used conventional analytical tools such as capillary electrophoresis. Subsequently, the employment of modern microfabrication technologies and materials since 1990s has enabled the capacity for generating complicated channel structures to realize versatile functions, making microfluidics a distinct field of research.¹ By geometrically constraining fluids into the sub-millimeter scale, microfluidics offers a physical environment largely different from

the macroscopic world, as a result of the significantly enhanced surface effects. This environment is characterized by the laminar flow and inertial particle behavior, short diffusion distance, and largely enhanced heat exchange. On the other hand, microfluidic systems can precisely confine and manipulate molecules/particles within a very small volume of liquid (10^{-9} to 10^{-18} l) and operate many functional units in parallel and in a programmed manner.² These characters empower microfluidic systems with the capacity of rapid, low-cost, and ultrasensitive analysis; high-throughput and automated operations; biomimetic functions; as well as various

30 October 2023 05:49:19

unique functions based on the special environment it creates.³ The recent two decades have witnessed the rapid advances of microfluidic technologies in various fields such as biotechnology;^{4,5} analytical science;^{6,7} and diagnostics;^{8,9} as well as physical, chemical,¹⁰ and biological research.¹¹ A number of nice reviews have been published to summarize the progress in these fields. On the other hand, one additional field is still emerging. With the advances in the nanomaterial and soft matter research, there have been some reports of the advantages discovered during attempts to synthesize these materials on microfluidic chips. As the formation of nanomaterials and soft matters is sensitive to the environment where the building blocks are fed, the unique physical environment of microfluidics opens up a lot of possibilities to form new products as compared to conventional bulk synthesis. However, related research has not fully excavated the potential of this field. This Perspective summarizes the recent progress in producing novel functional materials using microfluidics and discusses the trend of future development in this field. While the microfluidic synthesis of some specific types of products has been discussed elsewhere, the present Perspective is organized in the angle of different enabling powers of microfluidic synthesis originated from the unique physical environment. As summarized in Fig. 1, we structured the whole Perspective into five sections, each discussing one major enabling power, while within each section, we still divide the discussion by the different physical characters employed for special functions in the synthesis. We anticipate that this unique angle of organization not only serves for quickly summarizing the major means employed in microfluidic synthesis but also provides useful information to readers generally beyond the field of microfluidics about how and why microfluidics can provide new possibilities in synthesis, which may inspire their interest in trying out on their own reactions on the chip.

GENERATE PARTICLES WITH NARROW AND CONTROLLED SIZE DISTRIBUTION

Monodispersity is usually the desired character of a product in nanomaterial synthesis. In such synthesis processes, mixing often plays an important role since the local concentration of building blocks usually determines the structure formed as well as the rate of structure growth. The spatial heterogeneity of the reaction in solution often leads to deteriorated control in the range and distribution of the product size. In conventional bulk synthesis, controlling size distribution is often achieved by separation of nucleation and growth, while growth without additional nucleation is an effective condition for narrow size distribution of product particles.¹² Since microfluidics can employ different types of forces and effectively control the mixing condition within the micrometer scale, it has the chance to affect the size distribution of products too. In certain cases, this idea can be extended to the generation of polymers as well when monomers are considered the building blocks.

One way to improve monodispersity is to introduce highly localized fields to (actively) enhance mixing efficiency. For instance, Jiang *et al.* developed an alternating current electrothermal (ACET) micromixer-assisted approach for the synthesis of nanoparticles with narrow size distribution.¹³ Sequential micromixing was realized in this device by using pairs of asymmetrically staggered

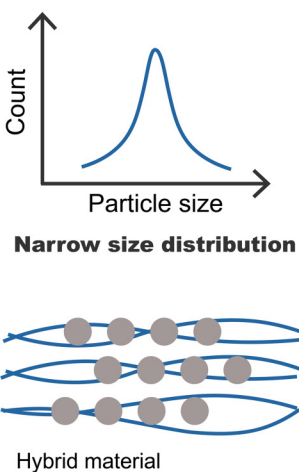
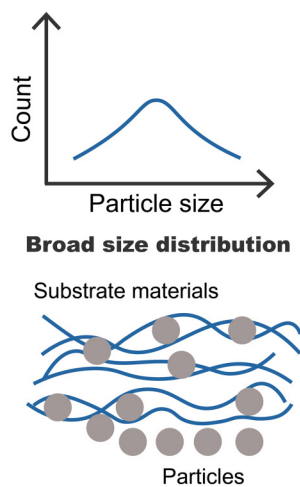
electrodes inside the microfluidic channel to form a three-fluid sequential mixing system as shown in Fig. 2(a). In this system, a body force is exerted on electrolytes by the ACET flow, which induces the fluid vortex motion to cause more efficient mixing between different fluids. The mixing condition is controlled by tuning the volume of fluids and voltage across the electrodes, which then affects the morphology and size dispersity of the synthesized nanoparticles. With the assistance of ACET, narrower size distribution (± 35.4 nm) of nanoparticles was achieved with a smaller mean particle size of 231.1 nm, as compared to the particles produced using the traditional method (352.9 ± 64.2 nm) [Fig. 2(a)]. Another example of active micromixing inside a microfluidic channel is electrohydrodynamic mixing. Tabrizian *et al.* utilized this approach to synthesize monodisperse nanoscale liposomes.¹⁴ As shown in Fig. 2(b), two liquid phases were quickly homogenized by the alternating electric field inside the microchannel. The authors discovered that by simply using 10 V_{pp} voltage, the micromixing was so effective that highly monodisperse liposomes could be produced at high flow rates up to 400 μ l/min. The authors also proposed that the two liquid phases in this system could also be a solvent and an antisolvent solution as the two phases of the nanoprecipitation systems; therefore, they believe the current approach is also applicable to the synthesis of nanoparticles. Meanwhile, acoustic mixing has also been employed to synthesize nanoparticles and nanomaterials in a controllable manner. Acoustic waves can transmit inside different types of media, making it effective to influence the processes at a distance from the emitter of the wave. On the other hand, not only the condition of the wave could be tuned by changing the emitter parameters but also the local condition could be affected by the geometry factors of the microchannel, making the acoustic-assisted methods flexible to create a desired environment for the reactions, i.e., enhanced mass transport of reagents at certain region inside a continuous liquid. In a work by Huang's group, reagent fluids were actively blended by the oscillation of sharp-edge structures in a microchannel, which facilitates rapid mass transport and thereby a complete mixing of reagents as shown in Fig. 2(c).¹⁵ The sharp edges of the channel structure inside an acoustic micromixer can create oscillating microbubbles, and the interfaces of both the sharp edges and the microbubbles can induce a fluid motion named acoustic microstream, which could enhance the local mixing.¹⁶ The synthesized nanoparticles of poly(lactic-co-glycolic acid)-polyethylene glycol (PLGA-PEG) on the acoustofluidic platform displayed a narrower size distribution than those prepared by bulk synthesis. Due to the flexible control of fluids by acoustics, the system can adapt the mixing constant by simply changing the acoustic streaming. Tabrizian's group has also delivered a similar idea to synthesis organic nanoparticles in an acoustic streaming system, with precise control of size and size distribution.¹⁷ Although there are advantages in active mixing, it is worth mentioning that heat generation might be an issue with the electric field or acoustic field. It might cause denaturation of biomolecules or changing of the reaction conditions. But this potential limitation could be effectively overcome by leveraging the nice heat dissipation capacity of microfluidic channels due to the large surface-to-volume ratio.¹⁸

In addition to active mixing, another strategy to achieve narrow and controlled size distribution is to better understand and

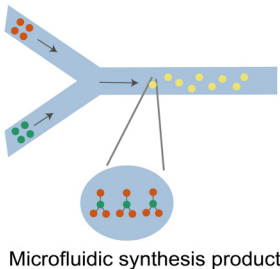
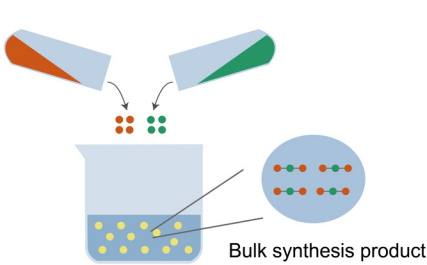
30 October 2023 05:49:19

Bulk Synthesis

Microfluidic Synthesis

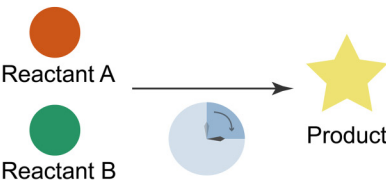
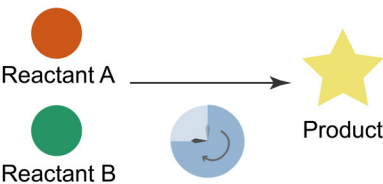


Hybrid materials unable to be synthesized Successful synthesis of hybrid materials



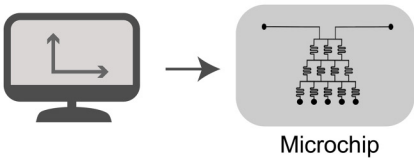
Synthesis of the conventional structure product

Synthesis of the new structure product



Normal reaction

Speed-up reactions



Manual operation

Automation

FIG. 1. Comparison between bulk synthesis and microfluidic synthesis. Compared to bulk synthesis, microfluidic synthesis has chance to produce nano/micro-particle products with narrower size distribution, hybrid materials with complicated structures, and products of new structures. Microfluidic systems can speed up operation and are more effective to realize atomization.

30 October 2023 05:49:19

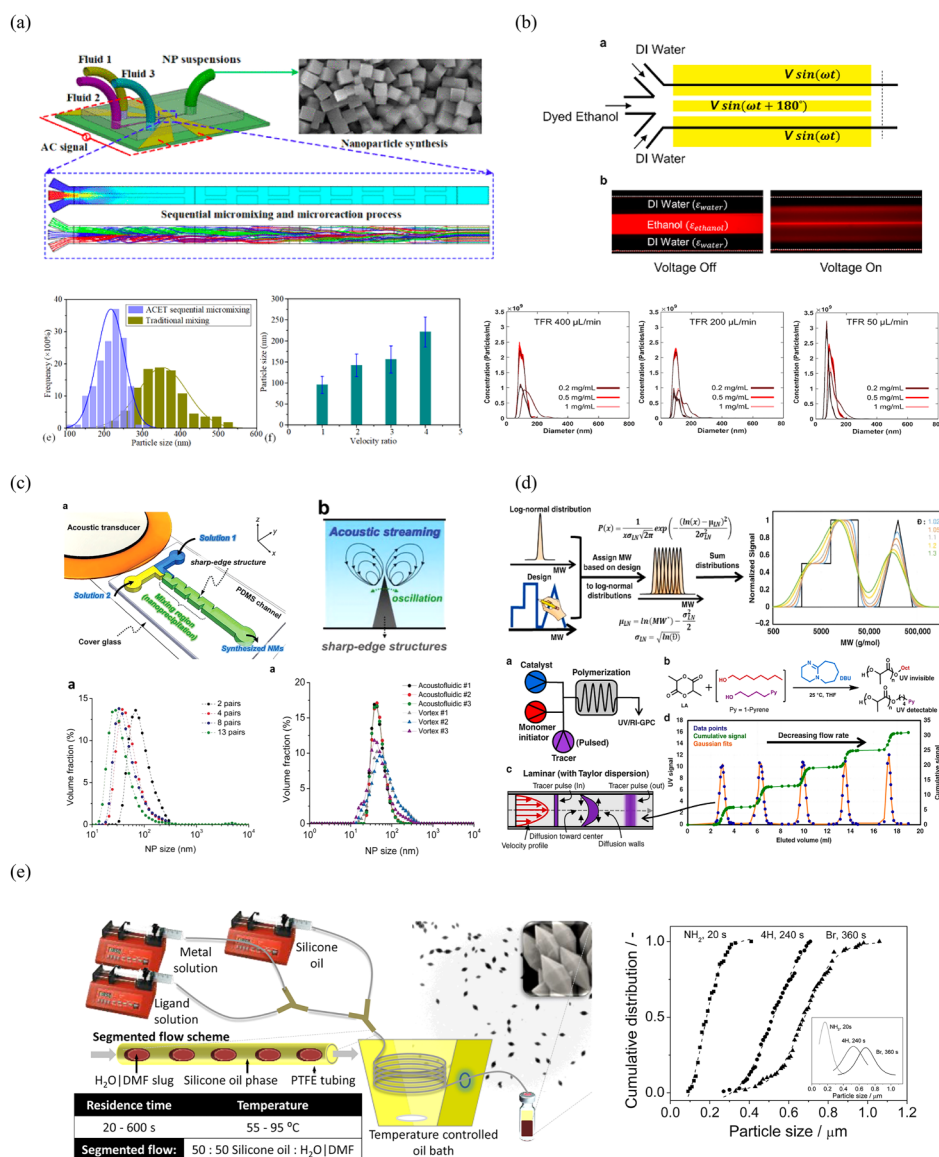


FIG. 2. Generate products with narrow and controlled size distribution. (a) Using alternating current electrothermal flow (ACET)-based active micromixing system to produce Co-Fe Prussian blue analog nanoparticles with a narrower size distribution compared to using the traditional method. Three pairs of asymmetrically staggered electrodes were placed inside the microfluidic channel to form a three-fluid sequential mixing system, which enables rapid mixing. Reproduced with permission from Sun *et al.*, Ind. Eng. Chem. Res. **59**, 12514 (2020). Copyright 2020 American Chemical Society. (b) Using an electrohydrodynamic micromixer to synthesis nanoscale liposomes with narrow size distribution. Electrodes were excited by voltages of the same amplitude (V) and frequency (ω) with the center electrode at a 180° phase shift. The mixing was switched by turning voltage on or off, which is indicated below the fluorescence images. Reproduced with permission from Modarres and Tabrizian, ACS Appl. Nano Mater. **3**, 4000 (2020). Copyright 2020 American Chemical Society. (c) Self-assembly of narrow-size-distributed PLGA-PEG NPs on the acoustofluidic platform. The sharp edges inside the microchannel are used for fluid mixing with the assistance of acoustic waves. When the acoustic transducer is off, an unmixed laminar flow pattern is observed, whereas a complete mixing of the two fluids is achieved when the acoustic transducer is on. Huang *et al.*, Adv. Sci. **6**, 1970113 (2019). Copyright 2019 Author(s), licensed under the Creative Commons Attribution (CC BY) License. (d) Flow reactor used for MWD control. Narrowly dispersed polymers are generated from the computer-controlled synthesis system to build large MWD. Operation conditions are controlled automatically by computer program based on the Taylor dispersion model and kinetic properties of the reaction. Dylan *et al.*, Nat. Commun. **11**, 3094 (2020). Copyright 2020 Author(s), licensed under the Creative Commons Attribution (CC BY) License. (e) Schematic of the microfluidic setup, segmented flow pattern, and synthesis details for MIL-88B type metal-organic frameworks. Cumulative particle size distribution of Fe-MIL-88B-NH₂ (95 °C, 20 s), Fe-MIL-88B (95 °C, 4 min), and Fe-MIL-88B-Br (95 °C, 6 min) are shown in the diagram. Dashed lines correspond to the fitting to a Boltzmann equation, with first derivatives in the inset. Reproduced with permission from Paseta *et al.*, ACS Appl. Mater. Interfaces **5**, 9405 (2013). Copyright 2013 American Chemical Society.

exploit the passive mixing inside microfluidic channels. Miscible fluids inside a microfluidic channel are usually in a laminar flow mode, of which the mixing effect is governed by diffusion and Taylor dispersion. Taylor dispersion is an effect that increases the effective diffusivity of a species inside a microchannel due to the presence of a shear flow. The heterogeneity of the flow rate along the channel radius broadens the bands of samples traveling inside a channel.¹⁹ While the former is determined by factors such as particle (molecule) size and temperature, the latter is affected by the channel geometry and flow characters. When these factors are well understood, one can predict the mixing conditions in the reaction environment and design appropriate strategies to generate desired products by coupling the mixing condition with the kinetic property of the reaction. Recently, Dylan *et al.* reported a solution to use a computer to control a microfluidic reactor and generate a polymerization product with desired molecular weight (MW) and molecular weight distribution (MWD).²⁰ They used the Taylor dispersion model and kinetic properties of the reaction to calculate the predicted MW and MWD in a T-junction reactor and used a computer to control the reactor's operation conditions. In this way, they not only can control the MW and MWD of a product but also enable an automated molecular sweep function to generate multiple MWs and different MWDs from the same set of starting materials [Fig. 2(d)]. In the meantime, their model provides a tool to explore the limits of any MWD design protocol. Moreover, the laminar flow environment could be tuned with additional factors such as temperature, pressure, and geometry confinement, which may further broaden the capacity of this model in supported reactions. As a representative work, Wang *et al.* reported a continuous-flow microfluidic synthesis approach, in which ultrafine (smaller than 2 nm) PtSn alloy nanoparticles were generated on the surface of various types of carbon supports (such as commercial carbon black particles, carbon nanotubes, and graphene sheets) carried by the laminar flow inside a heated and pressurized capillary tube.²¹ On the one hand, this design allows rapid and well-controlled heating and pressurization to the reactants as well as continuous generation of the products. On the other hand, the geometry confinement of the capillary enables a unique function compared to bulk synthesis. Limited by the diffusion rate in the laminar flow, the precursors have neglectable velocity relative to the carbon particles, making them quickly depleted through quasi-2D diffusion along the radial direction of the flow to the reaction sites on the carbon particles. In this way, starting with an appropriate concentration of the precursors in the liquid, this method can quickly form the desired nanocrystals of small sizes. In contrast to the laminar flow mode, segmented liquid–liquid flow (droplets) is another major mode of microfluidic reactors. Based on two immiscible fluids, droplet reactors provide an isolated environment that reduces contamination and clogging, while the liquid–liquid interface with a large relative surface area allows mass exchange and heat transfer. As one example, Joaquin's group reported a nanoliter reactor approach based on droplets in a microfluidic system.²² They were able to tune the crystal size and the width of the size distribution by changing the residence time and slug volume. They also found that a higher slip velocity yields a narrower particle size distribution because of enhanced internal mixing in the slugs [Fig. 2(e)].

GENERATE STRUCTURED HYBRID MATERIALS

While rapid mixing has been employed to generate products with narrow dispersity, the inherent “non-mixing” character of microfluidic flows is even more broadly used. This phase separation at the micrometer scale endows microfluidics with an intrinsic power to form hybrid materials with complicated structures for which the assembly of building units is guided by the interface. The “non-mixing” character is exhibited in two general types, depending on whether the involved liquids are miscible or not. When two immiscible liquids meet inside a microfluidic channel, they usually form segmented phases named plugs and droplets due to instability of the liquid interface, despite more strictly the droplet generation is governed by multiple parameters, such as the Reynold number, Capillary number, Weber number, Bond number, viscosity ratio, and flow rate ratio.²³ The plugs and droplets can serve as templates for generating functional materials, and the flexibility in choosing the reaction at the interface endows the generated particles/capsules with diverse characters. For example, Abell's group has reported an approach using droplets as templates to create ultra-thin supramolecular microcapsules.²⁴ They utilized the interface of the droplets to guide the host–guest or electrostatic assembly of molecules and were able to generate solid hydrogel microparticles, ultra-thin microcapsules, as well as core–shell microcapsules by changing the synthesis condition [Fig. 3(a)]. With the aid of this droplet platform, the generated capsules can be extremely monodisperse in size with broad compatibility of cargos. On the other hand, each droplet in a microfluidic system can also create an isolated and confined environment, in which unique reactions can take place. For instance, when Chen and his co-workers synthesized ZIF-8 [a type of metal–organic frameworks (MOF) particle of ca. 45 nm size] inside microdroplets containing graphene and carbon nanotubes (CNTs), they found the MOF particles not only grew on the (large) accessible graphene surfaces but also threaded with CNTs, resulting in a hierarchically hybrid nanomaterial.²⁵ It is noteworthy that the droplet interface itself can also serve as a unique two-dimensional site for the studies of orientation, packing, and aggregation behavior of molecules and particles that are sensitive to environmental conditions. As an example, de Pablo reported a computational study of the orientation behavior of liquid crystals on the interface of droplets.²⁶ The interface of droplets not only creates a confined environment to stabilize the particles for study but also establishes well controllable and differentiable conditions across the interface, offering a chance to precisely investigate the particles of interest. Moreover, the droplet-based reactions can be combined in a tandem fashion to generate core–shell particles by adding the reactants for the shell layer in the second step of the synthesis.²⁷

In contrast to the droplets mode, when two miscible non-viscous liquids meet inside a microfluidic channel, they usually form laminar flow due to the low Reynolds number. This laminar flow establishes a stable interface between two liquids over a considerably long scale, which enables the chance to form microstructured hybrid materials via reactions across the interface. For instance, Chen's team utilized laminar flow fabrication to produce different fiber-based materials for optical and energy-related applications. In one work, they utilized a laminar flow to introduce

30 October 2023 05:49:19

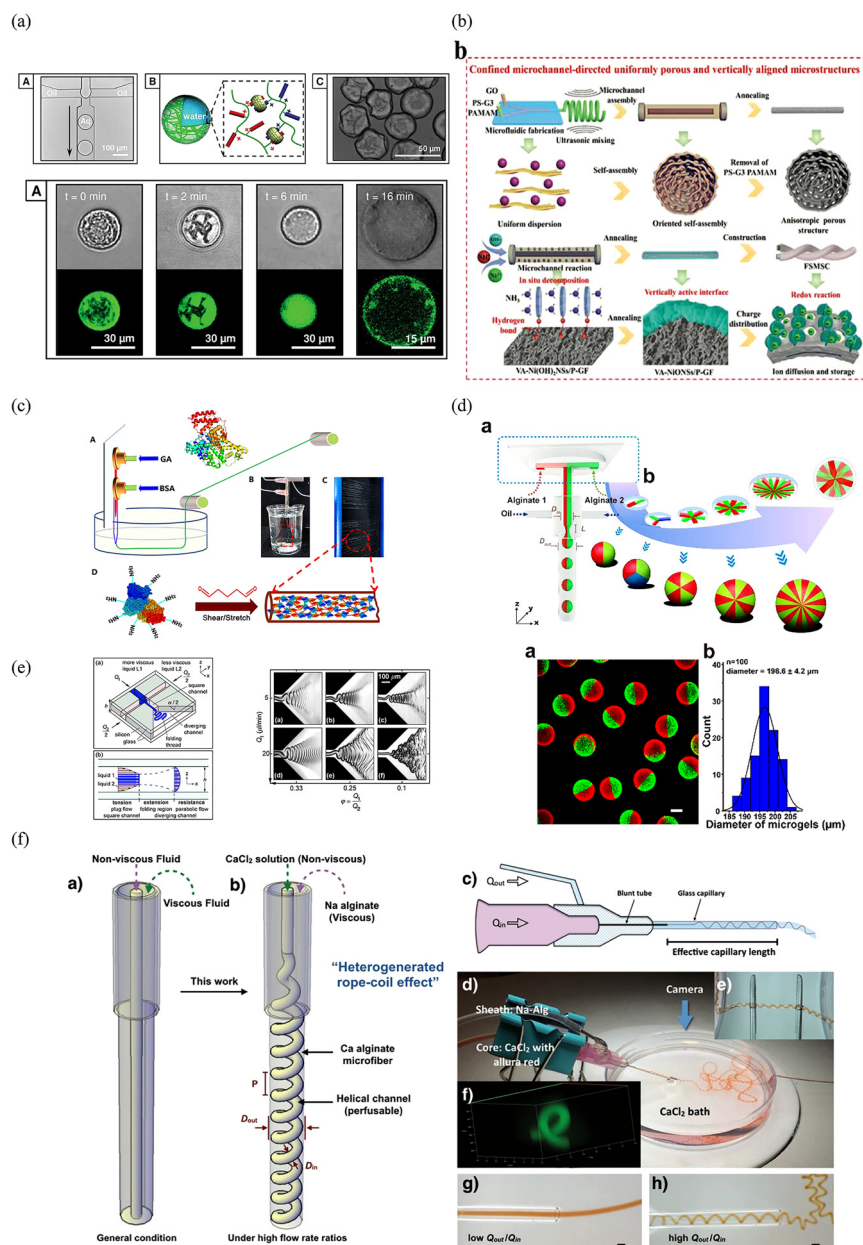


FIG. 3. Microfluidic systems to generate structured hybrid materials. (a) Assembly of solid hydrogel microparticles, ultra-thin microcapsules, as well as core-shell microcapsules guided by host-guest or electrostatic interactions at the interfaces of droplets. Different reactions at the interface endow the generated particles/capsules with diverse characters. Abell *et al.*, *Adv. Funct. Mater.* **25**, 4091 (2015). Copyright 2015 Author(s), licensed under the Creative Commons Attribution (CC BY) License. (b) Core-shell fiber VA-NiONS/P-GF formed in the laminar flow for energy storage. Sacrificial materials are applied to assist the laminar flow to produce uniformly porous anisotropic core-shell structures after removed. Meng *et al.*, *Adv. Sci.* **7**, 1901931 (2020). Copyright 2020 Author(s), licensed under the Creative Commons Attribution (CC BY) License. (c) Fabrication of BSA fiber by the microfluidic method. A coagulation bath and a rotation collector are built for coaxial laminar flow mixing. BSA protein and glutaraldehyde are crosslinked, dehydrated, and stretched in device to realize a fiber spinning process. Reproduced with permission from Liu *et al.*, *Angew. Chem., Int. Ed.* **59**, 4344 (2020). Copyright 2020 John Wiley and Sons. (d) Hydrogel microbeads are generated from a 3D microchannel system. The integrated chip-capillary droplet generator (ICCDG) is coupled with upstream chips to generate multi-compartmental particles. Reproduced with permission from Wu *et al.*, *Angew. Chem.* **132**, 2245 (2020). Copyright 2019 John Wiley and Sons. (e) Zigzag folding of a viscous flow stream inside a microfluidic channel. (f) Fabrication of microfibers with embedded helical channels based on the heterogenerated rope-coil effect. Microfibers with embedded straight and helical channels were generated, respectively, depending on the flow rate ratio. Reproduced with permission from Adv. Mater. **29**, 1 (2017). Copyright 2017 WILEY-VCH Verlag GmbH & Co. KGaA, Weinheim.

different types of reactants to form a coaxial core-shell fiber [Fig. 3(b)], which exhibits enhanced stability and robustness of halide perovskite nanocrystals for optoelectronic applications.²⁸ Note that each of the liquids in the laminar flow can also carry one or several types of particles, e.g., sacrificial templates for creating pores subsequently, and substances that may react upon changing the environment. Such character makes this approach powerful and versatile for generating complicated structures. For example, Chen *et al.* incorporated sacrificial template particles made of polystyrene during the formation of a self-assembly structure with the assistance of a laminar flow, and the subsequent removal of the sacrificial template particles created holes in the material, producing uniformly porous anisotropic core-shell structures based on nickel oxide arrays/graphene, which facilitates faster ion transportation kinetics.²⁹ This spirit has also been employed in another work to produce black phosphorus-hybrid microfibers for non-woven fabrics that might ultimately be useful to high energy density flexible supercapacitors.³⁰ Actually, this spirit of diffusive mixing can be extended to a broader regime, which might not contain a laminar flow. One example is that Nair, Jones, and their colleagues established a diffusive interface-based reactor by fixing a reactant-fed hollow fiber inside a reactant solution.³¹ This “interfacial microfluidic membrane” supports the diffusion of precursors across the porous wall to generate a framework through which a tubular structure can be formed. The diffusive reaction can even be originated from electrolyzing a solid material. As an instance, hydrogel capillary networks were generated from electrolyzing a copper template.³² On the other hand, the product of the laminar flow synthesis could be further treated using an external force. A case in point is the work of Liu *et al.*, where a coagulation bath and a rotation collector were used at the downstream of a coaxial laminar flow mixer.³³ In their work, BSA protein and glutaraldehyde were fed into the laminar flow mixer, and the cross-linking mixture was dehydrated in the coagulation bath and stretched by the rotation collector, realizing a fiber spinning process [Fig. 3(c)]. As a globular protein, BSA was generally not regarded as a good candidate for producing fibers, but because of the microfluidic shear force and post-stretching treatment, the BSA molecules were stacked in a long-range order, facilitating the close stacking and alignment of the BSA protein particles and, therefore, the formation of a highly tough fiber.³³ Finally, a laminar flow mixer can also be combined with a droplet generator to enable even more sophisticated functions. As a representative work, Lin *et al.* connected a horizontally placed laminar flow mixer with a vertically placed droplet generator to produce hydrogel microbeads with different internal compartments [Fig. 3(d)].³⁴ By varying the design of the two mixers, this 3D microchannel system could generate complicated particles that contain as many as 20 sub-compartments.

When two miscible liquids meet inside a microfluidic channel, including at least one viscous liquid within the two, another interesting phenomenon often takes place. If a more-viscous liquid is surrounded by a less-viscous liquid when injected into a microchannel, a folding process of the more-viscous stream is often triggered. Depending on the geometry of the microchannel, a zigzag folding³⁵ [Fig. 3(e)] or a rope coiling (spiral geometry) phenomenon may be observed, which could be exploited as a fabrication strategy. For instance, Zhao’s team created helical microfibers with

structures such as the novel Janus, triplex, core-shell, and even double-helix.³⁶ They proposed the potential use of these helical microfibers for magnetically and thermodynamically triggered microsprings, as well as for force indicators. Conversely, if a less-viscous liquid is surrounded by a more-viscous liquid when injected into a microchannel, normally a straight laminar flow will form. Nevertheless, Liang’s team recently discovered that when the flow rate ratio of the liquids is high, a rope-coil effect could still be reliably triggered, which they name the heterogenerated rope-coil effect [Fig. 3(f)]. They demonstrated the application of this effect in generating microfibers with embedded Janus channels and even double helical channels, as well as biomimetic supercoiling structures and perfusable/permeable spiral vessels.³⁷

GENERATE PARTICLES WITH NEW STRUCTURES

In addition to controlling the size and composition of the product, microfluidic platforms can also generate particles with structures hard to synthesize in the bulk solution, which may consequently enable new functionality of the material. While reported strategies share a common foundation of mechanism—to leverage the heterogenic distribution of reactants created by microfluidic technologies, these methods can be generally classified into active and passive approaches. As one type of active approach, acoustic technology has been used to create products with unique structures. A useful function of acoustomicrofluidics is well-controlled nebulization, which can enable unique evaporation conditions that lead to novel products and is friendly to heat-sensitive substances. For example, Yeo *et al.* demonstrated an acoustomicrofluidic nebulization technique that can access intermediate evaporation rate regimes (10^{-5} to 10^{-6} l/h)—between the conventional slow solvent evaporation (10^{-11} to 10^{-12} l/h) and fast spray drying (10^{-1} l/h)—and thereby capable of producing novel crystal morphologies [Fig. 4(a)].³⁸ It is well known that the crystallinity, crystal size, and size distribution are all highly dependent on the evaporation rate. As a result, new crystallization morphologies of sodium chloride and glycine, respectively, were observed in their work. Moreover, the authors believe the system has better power efficiency than conventional spray dryers. As another example, Esther’s group developed a surface acoustic wave-based spray-dryer, which can produce droplets with diameters of only a few micrometers.³⁹ The small droplet size triggers highly fast evaporation, which kinetically suppresses the crystallization of solutes and results in amorphous particles. Another application of the surface acoustic wave is to modulate the spatial distribution of reactants. In a representative work, Yeo *et al.* utilized a thin resonant acoustowetting film to confine the precursors of MOF synthesis, which arrests further crystal growth in thickness and resulted in a large aspect ratio MOFs (30–50 nm thin, 10 μ m wide, and 100 μ m long) swordlike morphologies.⁴⁰ While the method can control the thickness of the product through the pulse modulation of the acoustic excitation, the ultrathin MOF architecture is believed to facilitate the exposure of its inherently hidden metal active sites.

Regarding the passive approaches, laminar flow reactors are good examples. Compared to bulk synthesis methods, a notable feature of laminar flow reactors is the diffusive mixing as a result of the low Reynolds number. Despite being well predictable and

30 October 2023 05:49:19

controllable, the diffusive mixing in a liquid flow, even within a small scale, is not always quicker than an agitated mixing in a bulk reactor; in fact, it is often slower than the latter when the radius of the flow is not very small. This, in turn, may lead to new structures of the products. For example, such a mixing environment might affect the crystallinity of the synthesized particles and create porous structures in materials generated upon mixing. In our recent work, we discovered that the continuously changed concentrations of MOF precursors in the gradient mixing on-chip resulted in structural defects in products, which gives rise to mesopores in MOFs [Fig. 4(b)].⁴¹ Thus, while the as-produced enzyme-MOF composites still maintain the protection to the enzymes as those from conventional bulk solution synthesis, they showed much higher (~one order of magnitude) biological activity than the latter due to the improved access of substrates to the encapsulated enzymes. In contrast, it was reported that the fast mixing in droplet-based MOF synthesis led to a high level of crystallinity with no defect in the material. Compared to existing strategies for generating mesopores that usually use templates and are thus complicated with the risk to damage enzyme activity during the template removal processes, our method generates the mesopores spontaneously during the single-step preparation of particles without using any template. Interestingly, when the flow media is changed, laminar flow mixing is not always slow even if the radius is not very small; accordingly, the controllable laminar flow may generate defect-free crystal structures. As a representative work, Aymonier *et al.* demonstrated a laminar flow microfluidic reactor based on supercritical fluid and used it to synthesize exciton luminescent ZnO nanocrystals. ZnO nanocrystals synthesized through liquid-phase reactions are often rich in defects, which cannot serve as exciton emitters [Fig. 4(c)].⁴² Since the mass transfer character of a supercritical fluid can be closer to that of a gas, this reactor produced defect-free ZnO particles just like these from gas-phase reaction and yet can control the size distribution of the particles taking advantage of the microfluidic synthesis. Last but not least, the shear stress inside the laminar flow itself can contribute to the formation of different particles via self-assembly, especially for those based on weak interactions, e.g., the “soft” protein corona. When nano- and micro-sized particles are exposed to a biological fluid, biomolecules such as proteins will adsorb on the particle surface and form a protein shell, named “corona,” which has attracted great attention in pharmaceuticals and diagnostics. Usually, the protein coronas are considered to form in two stages, which are also called the evolution of the corona. In the first stage, a “hard” corona is generated quickly through the adsorption of proteins with high affinity to form a tightly bound layer. In the second stage, a cloud of loosely bound proteins is formed as the outer shell, often referred to as the “soft” corona. Largely depending on the intrinsic character of the particles, either two stages or only the soft corona will take place. While external conditions (e.g., channel structure, liquid composition, flow velocity) would not play a major role in determining whether a hard corona will form, they will significantly affect the structure and composition of the soft corona.⁴³ Notably, the formation of these self-assemblies is inherently dynamic, depending not only on the pristine particles and the composition of the biological fluids, but also on the shear stress environment, which is particularly crucial to the composition and structure of the “soft” corona. The microfluidic system is

inherently fitted to mimic the hydrodynamic environment of the *in vivo* condition. By employing different channel structures and changing the velocity of flow, the dynamic formation of protein coronas can be effectively studied [Fig. 4(d)].^{44–46}

COMPLETE REACTIONS WITH THE QUICKER RATE AND A NEW REACTION ROUTE

The high surface-to-volume ratio and small dimension for mass and heat transfer endow microfluidic systems with unique capabilities to complete some reactions at significantly quicker rates. For example, Yan’s team reported a voltage-controlled interfacial microreactor that can accelerate electrochemical reactions.⁴⁷ This reactor is formed at the solution–air interface of the Taylor cone in an ESI emitter with a large (139 μm) orifice at a low ESI flow rate (a few tens of nl/min), which allows the continuous contact of the electrode and reactants right before leaving the Taylor cone and sprayed into air, while the reacting droplets emitted from the orifice are immediately detected by the MS, quickly enough to study the reaction mechanisms by detecting transient intermediates [Fig. 5(a)]. Compared to the corresponding bulk reactions, a roughly two-order acceleration in reaction rates was observed when this reactor was used for the electro-oxidative C–H/N–H coupling of DMA and PTA, as well as electrochemical derivatization of benzyl alcohol. Moreover, the authors discovered that the reaction acceleration was mainly at the interface of the Taylor cone rather than in the electrosprayed microdroplets. However, it is noteworthy that in some other reactions, the accelerated rate is indeed observed inside the droplets. Extensive investigations have suggested various mechanisms of the accelerated reaction rate, such as partial solvation of reactants (enthalpy effect), ordered orientation (entropy effect), fast diffusion, mixing, and solvent evaporation.⁴⁸ Just to raise one example, using a droplet-assisted reaction platform, Kim *et al.* synthesized zeolite nanoparticles (ZSM-5) within 15 min, which would take several hours via bulk reactions.²⁷ In addition to the enhanced mixing and heat transfer, which are considered responsible for the accelerated reaction, the authors observed that the aging of the synthesizing solution was much faster (20-min aging in the droplets equals 5 h in the bulk phase), which may affect the level of the crystallinity of the products. Similarly, generally two-order faster kinetics than bulk solution synthesis was observed when Kim *et al.* used the droplet reaction platform to prepare representative MOF structures (e.g., HKUST-1, MOF-5, IRMOF-3, and UiO-66) via solvothermal approaches.⁴⁹

Other than accelerating reactions, microdroplets may even trigger reactions not existent in the bulk solution.⁵⁰ For example, Zare’s team recently conducted a series of experiments based on water microdroplets generated through atomizing bulk pure water or condensing water vapor from air and discovered hydrogen peroxide at the concentration of tens of micromolar.^{51,52} For comparison, commercial hydrogen peroxide is produced through the anthraquinone oxidation (AO) process, which can hardly be considered a green method.⁵³ Since no catalyst, electric field, or light was employed in the Zare team’s experiments, they suggested that hydrogen peroxide was generated through a spontaneous oxidation process via hydroxyl radical recombination, which took place

30 October 2023 05:49:19

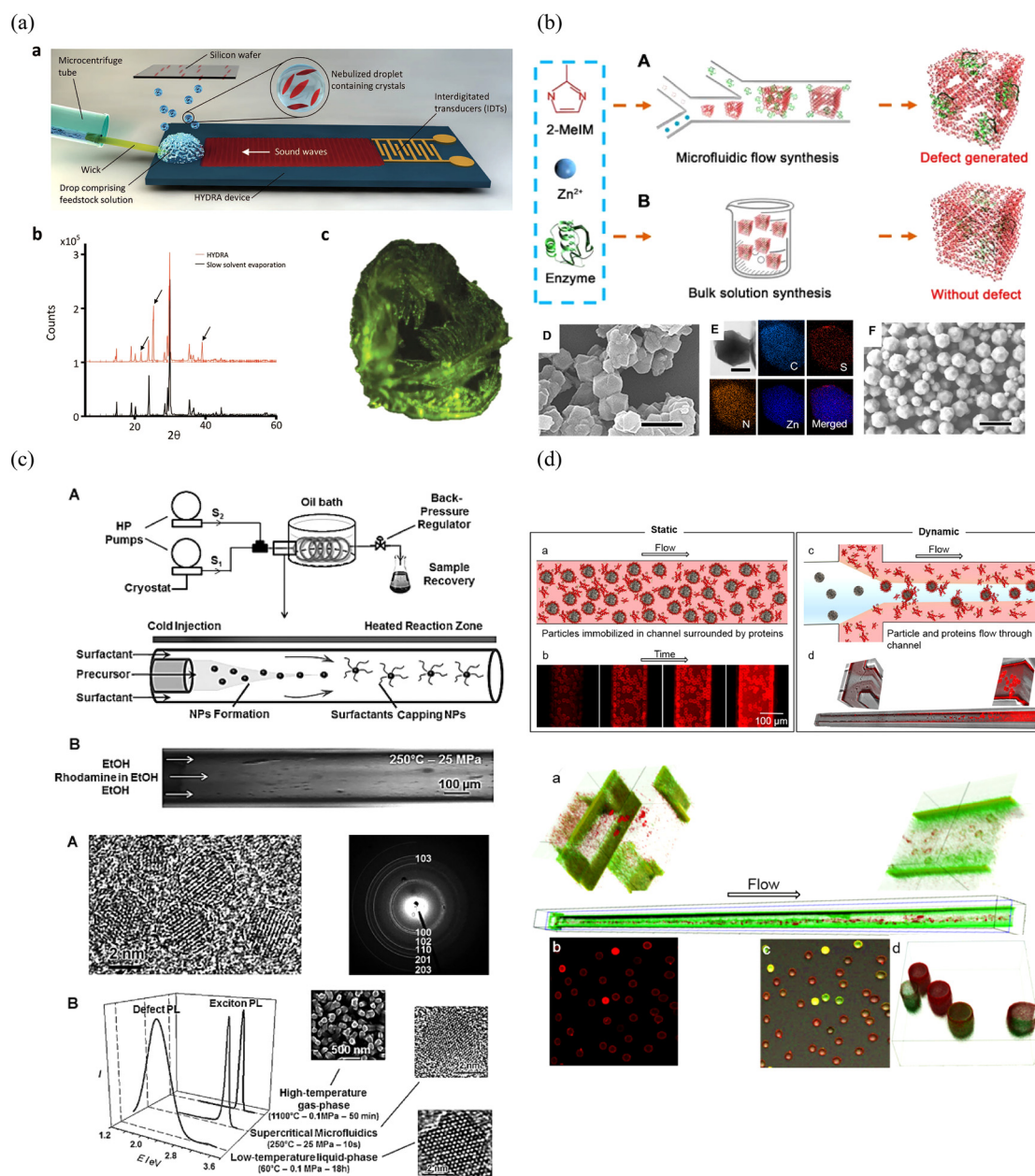


FIG. 4. Microfluidic systems to generate particles with new structures compared to those from bulk synthesis. (a) Metal-organic frameworks (MOFs) with unique swordlike morphologies (30–50 nm thin, 10 μ m wide, and 100 μ m long) are produced by a thin resonant acoustowetting film to arrest further growth of the crystal. Pulse modulation is applied to control the thickness of the products. Reproduced with permission from Ahmed *et al.*, *Adv. Mater.* **30**, 1602040 (2018). Copyright 2017 John Wiley and Sons. (b) Defect-rich enzyme-MOF composites are produced in a microfluidic gradient mixing system. Structural defects are spontaneously created in these MOFs, which provides mesopores for better mass transfer. While maintaining their protection to the enzymes, these MOFs show a much higher biological activity compared to those synthesized conventionally with bulk solution approaches. Hu *et al.*, *Sci. Adv.* **6**, 1 (2020). Copyright 2020 Author(s), licensed under the Creative Common Attribution (CC BY) License. Reproduced with permission from Roig *et al.*, *Angew. Chem., Int. Ed.* **50**, 12071 (2011). Copyright 2022 John Wiley and Sons. (c) Protein corona formation in the microfluidic system under static and dynamic conditions, respectively. 3D PDMS chip with a cross-shaped mixer geometry is used for focusing the silica particles in the central stream and fluorescently labeled proteins. The green signal indicates that HSA-Cy3 can attach to the surface of the particles during traveling inside the channel. Reproduced with permission from Weiss *et al.*, *ACS Appl. Mater. Interfaces* **11**, 2459 (2019). Copyright 2019 American Chemical Society.

inside an intrinsic electric field at the air–water interface of the microdroplets.⁵⁴ Meanwhile, the electric double layer is not limited to the air–water interface; with the assistance of stimulated Raman excited fluorescence microscopy, an electric field as strong as 10^7 V/cm was also observed at the oil–water interface. Meanwhile, theoretical analysis based on the three-dimensional Gouy–Chapman model also predicted a strong concentration of charged molecules toward the surface of the droplet and generally suggested that such a character will gradually disappear when the size of the droplets grows beyond $10\ \mu\text{m}$, which is consistent with the observation in experiments.⁵⁵ One interesting aspect is that in the prediction result, the electric double layer penetrates deeply into the droplet much farther than that would be predicted by the one-dimensional Gouy–Chapman model, which might be a reason that such an effect was paid less attention to before. This discovery in droplet-size-enhanced reactivity opens up promising possibilities in potential new microfluidic technologies. Finally, the carrier phase surrounding the droplets can create a unique environment for the droplet-based reactions too. For example, in the work of Kim *et al.*, ionic liquids were used as the continuous phase in a droplet-based synthetic approach for generating zeolite particles.²⁷ The utilization of ionic liquids not only creates thermally stable (e.g., 150°C) and nonvolatile environment but also offers templating function for some reactions. In this way, materials difficult to synthesize via the conventional bulk solution approach might be easily generated inside microfluidic channels.

ENABLE MORE EFFECTIVE AND EFFICIENT CONTROL ON REACTIONS

On top of the above functions, the convenience and flexibility in manipulating small amounts of liquids and integrating different elements (e.g., light, heat, and the electric field) into the operation environment make microfluidic systems advantageous for controlling reactions in more effective and efficient ways. Stated differently, microfluidic systems can improve the yield and selectivity of reactions, reduce the reagent and labor cost, and enhance the throughput of operations. A frequently utilized character of microfluidics is the large surface-to-volume ratio, which creates useful room to introduce functional elements at the interfaces. One example is that active sites for reactions such as enzymes can be immobilized on the surface of microchannels to establish a reactor for continuous production. Enzyme immobilization is an extensively investigated technology, which can significantly enhance the stability and reusability of enzymes. However, the efficiency in mass transfer has frequently been a challenge in some enzyme immobilization strategies due to the blockage by the immobilization solid framework. When enzymes are immobilized on the surface of a microfluidic channel, on the other hand, this mass transfer challenge may be largely addressed, and the reusing efficiency can be improved as well since the reactor can be operated in the continuous flowing mode. In this way, the enzyme-immobilized microchannel itself serves as a functional material. We demonstrated that when D-ribulose-1,5-bisphosphate carboxylase/oxygenase was immobilized on the surface of a microfluidic channel, enhancement was observed in both enzyme stabilities (7.2 folds in storage stability and 6.7 folds in thermal stability) and reusability

(90.4% activity retained after five cycles of reuse and 78.5% after ten cycles).⁵⁶ In addition to cost efficiency, microfluidic platforms can also significantly improve efficiency and convenience in operation, which is particularly useful for complicated and high-throughput processes.

One effective way to improve the operation efficiency is to digitize the fluid into droplets, which can be manipulated via serial/parallel operations. Different strategies can be used to manipulate the droplets. For example, Huh *et al.* demonstrated the synthesis of cesium lead halide perovskite nanocrystals based on a serial droplet reaction system, which consists of two cross-shape microfluidic junctions and a heating block.⁵⁷ Droplets containing the precursors of perovskite are generated in the first junction; during the transfer of these droplets to the second junction, the velocity gradient of the carrier flow induces a recirculating flow inside each droplet, which enhances the mixing of the precursors [Fig. 5(b)].⁵⁸ At the second junction, the stepwise anion-exchange reaction is initiated, after which the droplets pass through a heating zone to generate nanocrystals. By changing the ratio of flowrates at the two junctions, the system can generate a product with the tunable color of fluorescence in the entire visible range.⁵⁹ In addition to solely hydrodynamic and intrinsic surface energy, electro-wetting of droplets has been broadly used to realize more complicated operations, which is often named digital microfluidics. By applying a series of electrical potentials to an array of electrodes coated with a hydrophobic insulator, a digital microfluidic device can effectively control multiple droplets independently to realize operations such as moving, merging, mixing, splitting, or dispensing from reservoirs, which helps one to accomplish sophisticated processes in an automatic and high-throughput manner. As a representative work, Wheeler's team demonstrated the synchronized synthesis of peptide-based macrocycles by digital microfluidics.⁶⁰ In their system, ten reagent reservoirs and 88 actuation electrodes were used to realize the multistep synthesis, which was capable of forming five products in parallel [Fig. 5(c)]. Owing to its open droplet nature, a unique feature of digital microfluidics is that it supports solvent removal and re-dissolution of solid products for further processing. The products formed on the device of digital microfluidics can be subsequently analyzed by some instruments (e.g., by simply removing the top plate of the device). In this way, digital microfluidics can be a good choice for fast and automated synthesis of libraries of compounds for applications such as drug discovery and high-throughput screening. It is worth mentioning that electrowetting can be combined with surface engineering to further enhance the flexibility and throughput of the operation. For instance, Lammertyn, Sels, and their teammates reported a platform for high-throughput printing of monodispersed single MOF crystals into uniform arrays on a flat surface. In their work, they replaced the top plate of a typical digital microfluidic device with a plate containing hydrophilic-in-hydrophobic micropatches $10\text{--}50\ \mu\text{m}$ in size.⁶¹ When the “mother” droplets containing MOF precursors are manipulated by the bottom plate as a typical electrowetting system, femtoliter droplets are dispensed into the micropatches due to the selective wettability. In this way, they can print thousands of microdroplets onto the top plate within only a few seconds using only four actuation electrodes. With the aid of evaporation, each femtoliter microdroplet will be converted into a single

30 October 2023 05:49:19

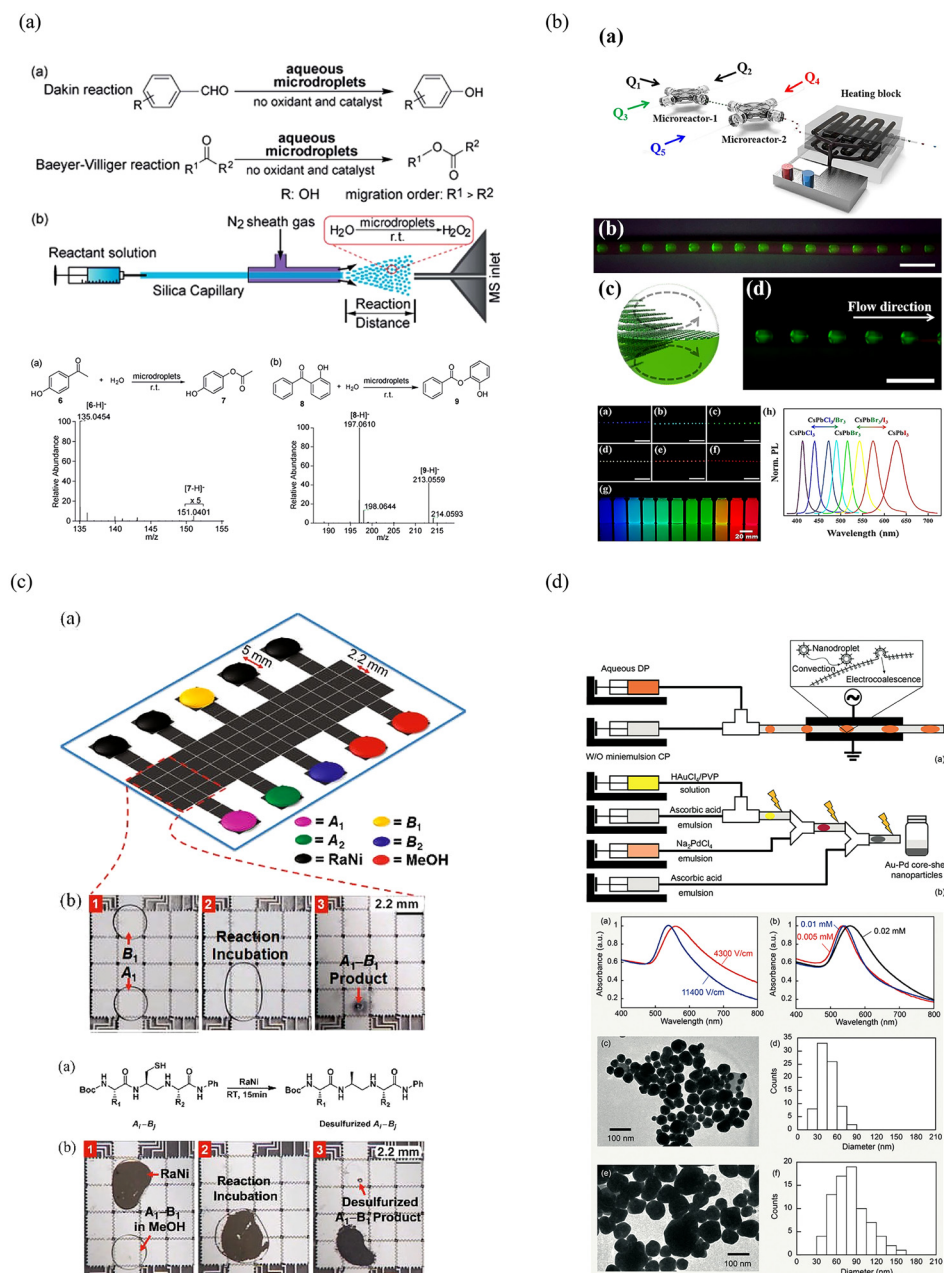


FIG. 5. Microfluidic systems that accelerate reactions and provide new reaction routes. (a) Ketones and ester compounds synthesized by Dakin and Baeyer–Villiger reactions in catalysts-free aqueous microdroplets. Spontaneous oxidation process via hydroxyl radical combination has formed an intrinsic electric field at the air–water interface of the microdroplets, which makes many reactions more efficient and effective. Reproduced with permission from Cheng *et al.*, *Angew. Chem., Int. Ed.* **59**, 19862 (2020). Copyright 2022 John Wiley and Sons. (b) Droplet-based microfluidic strategy to synthesize $CsPbX_3$ ($X = Br$) perovskite NCs. Velocity gradient of the carrier flow induces a recirculating flow inside each droplet to enhance the mixing of the precursors. Reproduced with permission from Kang *et al.*, *Chem. Eng. J.* **384**, 123316 (2020). Copyright 2020 Chemical Engineering Journal. (c) A digital microfluidic method for combinatorial chemical synthesis of peptidomimetics and related products. Digital microfluidic synthesis of peptide-based macrocycles is realized by using eighty-eight actuation electrodes to allow the formation of five products in parallel. Reproduced with permission from Jebail *et al.*, *Angew. Chem.* **122**, 8807 (2010). Copyright 2010 John Wiley and Sons. (d) W/O miniemulsion and electrocoalescence ways to generate aqueous microdroplets in the microfluidic system. Voltage can be self-adjusted by alternating the integrated miniaturized actuators, providing effective and versatile control of the microdroplets and reactions within small dimensions. Hatton *et al.*, *Lab Chip* **18**, 1330 (2018). Copyright 2018 Author(s), licensed under the Creative Commons Attribution (CC BY) License.

crystal with a high success rate. They found that the generated single crystals are highly monodispersed, presumably owing to the uniform size of the droplets. The patterned surface wettability could be combined with other force fields too, even including gravity to manipulate droplets on a surface, which allows extended flexibility in the device design and functionality.⁶²

In addition to the on-surface scheme, the in-channel scheme is also frequently employed to realize automated and high-throughput operations. While the utilization of the continuous

phase enables a very high speed and throughput of operation, one key challenge to the application of in-channel droplet-based microfluidic systems is how to add new chemicals to the droplets for subsequent reactions. Various strategies have been developed for this purpose, such as hydrodynamic droplet merging (e.g., based on the in-phase meeting of droplets from two streams or based on the phenomenon that smaller droplets travel slower than large droplets in the same stream),⁶³ direct injection (which uses a side channel to directly inject aqueous reagent into flowing droplets),⁶⁴

electro-coalescence (which merges pairs of droplets by applying an electric field),⁶⁵ and their combinations.⁶⁶ While most of the strategies require synchronization in control and offer a limited dynamic range of the mixing ratio, it is worth noting that precise yet convenient addition of chemicals into droplets with a wide range of mixing ratios is available based on some designs. Hatton *et al.* demonstrated that when a W/O miniemulsion (or called nanoemulsion) is used as the continuous phase, the addition of chemicals into droplets can be realized through electrocoalescence with the precise control of both the amount and the rate.⁶⁷ A miniemulsion is a thermodynamically metastable system with nanodroplets (e.g., 50–500 nm in size) dispersed in an immiscible solvent. When an alternating electrical field is applied, chemicals carried by aqueous nanodroplets can be transferred to the aqueous droplets carried in the miniemulsion at a wide range of controllable rates, realizing a “quasi-continuous” addition of chemicals into the droplets inside the channel [Fig. 5(d)]. Accordingly, this approach is less dependent on precise synchronization in control. Last but not least, as exemplified in different sections above, the flexibility in integrating miniaturized actuators to create effective and versatile control of the localized environment within small dimensions further extends the functionality of microfluidic systems in complexed synthesizing approaches.

CONCLUSIONS

Over approximately three decades since its debut, microfluidics has gained attention more as an enabling tool to create new analytical technologies, as compared to other potential roles. Nevertheless, microfluidics has never lost its promise in creating new routes and new means for synthesizing materials that are otherwise difficult to produce. This promise originated from some inherent characters of microfluidic systems, such as fast and precisely controllable mass and heat transfer, largely enhanced interface effect, confinement effect, templating effect, low-Reynolds number flow behavior, flexibility in coupling with different types of actuators and physical fields, versatile and effective control of the highly localized environment, and convenience in integrating different functional modules into an automatic system. As a result, microfluidic technology can enable various helpful new functionalities in synthesizing functional materials, including but not limited to enhancing reaction rate and operation efficiency, generating particle products with better monodispersity, producing hybrid materials with complex pre-designed structures, creating materials otherwise difficult to synthesize, and completing reactions with new reaction routes. Quite a portion of these functionalities is still underexplored, leaving large room for new possibilities. Particularly, microfluidics holds nice potential to become an important source of creating new functional materials. Nevertheless, there remain some hurdles to the broader implementation of microfluidic synthesis. An important one is how to scale up the production. For some of the approaches, this issue exists simply for the need of research purpose—these approaches might struggle to provide a sufficient amount of product for analysis purposes. The limitations in scaling up could be attributed to multiple reasons. For example, some of the approaches use a lot of solvents to carry

the reactants; it might become an issue how to effectively recover the products and recycle the solvents for the sake of cost efficiency. On the other hand, in some approaches, the products (as particles) may stick to the channel wall and finally clog the channel, limiting the possible duration of production. This issue is tied to a fundamental character of microfluidic systems in which surface effects are amplified and thus materials for making the device play an important role in its functionality.⁶⁸ Researchers including our team have been making efforts on addressing these fouling-related issues for over a decade too.^{69–71} Finally, the fabrication and manufacturing process of microfluidic devices may sometimes be challenging for various applications. The most commonly used material for making microfluidic devices, PDMS, is well known for its incompatibility with solvents, largely limiting its implementation in on-chip synthesis. Similarly, the materials used for making disposable bioassay devices, such as polystyrene (PS) and poly(methyl methacrylate) (PMMA), as well as 3D printed materials, are prone to either solvent dissolution/swelling or molecular leaching. On the other hand, the solvent-resistant materials, such as silicon, glass, quartz, and stainless steel, are expensive to microfabricate and difficult to integrate on-chip valves. Our team reported some thermal molding methods to mass-produce inexpensive solvent-resistant microfluidic chips using materials such as polypropylene (PP) and Teflon.^{69,70} These microchips could be suitable choices for some on-chip reactions, but they are still not ideal platforms to incorporate on-chip valving. With the possibility of conveniently scaling up the microfluidic synthesis, we anticipate a wave of rapid advances in microfluidic-based technologies for creating new functional materials.

ACKNOWLEDGMENTS

This work was supported by NSFC (Nos. 51773173 and 81973288), HKRGC (Nos. 12301720, T12-201/20-R, RMGS 2020_4_01, and PDFS2021-2S02), and SZSTC (No. SGDX20190816230207535).

AUTHOR DECLARATIONS

Conflict of Interest

The authors have no conflicts to disclose

Author Contributions

Xinying Xie: Conceptualization (lead); Funding acquisition (lead); Supervision (lead); Writing – original draft (equal); Writing – review & editing (equal). **Yisu Wang:** Writing – original draft (supporting); Writing – review & editing (supporting). **Sin-Yung Siu:** Writing – original draft (supporting); Writing – review & editing (supporting). **Chiu-Wing Chan:** Writing – original draft (supporting); Writing – review & editing (supporting). **Yujiao Zhu:** Writing – review & editing (supporting). **Xuming Zhang:** Writing – review & editing (supporting). **Jun Ge:** Writing – review & editing (supporting). **Kangning Ren:** Conceptualization (lead); Funding acquisition (lead); Supervision (lead); Writing – original draft (equal); Writing – review & editing (lead).

DATA AVAILABILITY

Data sharing is not applicable to this article as no new data were created or analyzed in this study.

REFERENCES

- ¹A. J. DeMello, *Nature* **442**, 394–402 (2006).
- ²G. M. Whitesides, *Nature* **442**, 368–373 (2006).
- ³Y. Song, J. Hormes, and C. S. S. R. Kumar, *Small* **4**, 698–711 (2008).
- ⁴L. Y. Yeo, H. C. Chang, P. P. Y. Chan, and J. R. Friend, *Small* **7**, 12 (2011).
- ⁵Y. Ai, R. Xie, J. Xiong, and Q. Liang, *Small* **16**, e1903940 (2020).
- ⁶Q. Zhang, S. Feng, L. Lin, S. Mao, and J. M. Lin, *Chem. Soc. Rev.* **50**, 5333 (2021).
- ⁷D. G. Rackus, M. H. Shamsi, and A. R. Wheeler, *Chem. Soc. Rev.* **44**, 5320 (2015).
- ⁸P. Yager, T. Edwards, E. Fu, K. Helton, K. Nelson, M. R. Tam, and B. H. Weigl, *Nature* **442**, 412 (2006).
- ⁹L. Mathur, M. Ballinger, R. Utharala, and C. A. Merten, *Small* **16**, 1904321 (2020).
- ¹⁰Q. Zhao, H. Cui, Y. Wang, and X. Du, *Small* **16**, 1 (2020).
- ¹¹K. N. Han, C. A. Li, and G. H. Seong, *Annu. Rev. Anal. Chem.* **6**, 119 (2013).
- ¹²J. Park, J. Joo, S. G. Kwon, Y. Jang, and T. Hyeon, *Angew. Chem., Int. Ed.* **46**, 4630 (2007).
- ¹³H. Sun, Y. Ren, Y. Tao, T. Jiang, and H. Jiang, *Ind. Eng. Chem. Res.* **59**, 12514 (2020).
- ¹⁴P. Modarres and M. Tabrizian, *ACS Appl. Nano Mater.* **3**, 4000 (2020).
- ¹⁵P. H. Huang, S. Zhao, H. Bachman, N. Nama, Z. Li, C. Chen, S. Yang, M. Wu, S. P. Zhang, and T. J. Huang, *Adv. Sci.* **6**, 1970113 (2019).
- ¹⁶A. Hashmi, G. Yu, M. Reilly-Collette, G. Heiman, and J. Xu, *Lab Chip* **12**, 4216 (2012).
- ¹⁷M. R. Rasouli and M. Tabrizian, *Lab Chip* **19**, 3316 (2019).
- ¹⁸Y. Liu, N. Wang, C. W. Chan, A. Lu, Y. Yu, G. Zhang, and K. Ren, *Front. Cell Dev. Biol.* **9**, 1 (2021).
- ¹⁹B. J. Kirby, *Micro-and-Nanoscale Fluid Mechanics: Transport in Microfluidic Devices*. (Cambridge University Press, 2010).
- ²⁰D. J. Walsh, D. A. Schinski, R. A. Schneider, and D. Guirounet, *Nat. Commun.* **11**, 3094 (2020).
- ²¹F. Wu, D. Zhang, M. Peng, Z. Yu, X. Wang, G. Guo, and Y. Sun, *Angew. Chem., Int. Ed.* **55**, 4952 (2016).
- ²²L. Pasetta, B. Seoane, D. Julve, V. Sebastián, C. Téllez, and J. Coronas, *ACS Appl. Mater. Interfaces* **5**, 9405 (2013).
- ²³P. Zhu and L. Wang, *Lab Chip* **17**, 34 (2017).
- ²⁴R. M. Parker, J. Zhang, Y. Zheng, R. J. Coulston, C. A. Smith, A. R. Salmon, Z. Yu, O. A. Scherman, and C. Abell, *Adv. Funct. Mater.* **25**, 4091 (2015).
- ²⁵H. Cheng, J. Meng, G. Wu, and S. Chen, *Angew. Chem., Int. Ed.* **58**, 17465 (2019).
- ²⁶J. A. Moreno-Razo, E. J. Sambriski, N. L. Abbott, J. P. Hernández-Ortiz, and J. J. De Pablo, *Nature* **485**, 86 (2012).
- ²⁷P. H. Hoang, H. Park, and D. P. Kim, *J. Am. Chem. Soc.* **133**, 14765 (2011).
- ²⁸J. Meng, G. Wu, X. Wu, H. Cheng, Z. Xu, and S. Chen, *Adv. Sci.* **7**, 1901931 (2020).
- ²⁹X. Lu, Y. Hu, J. Guo, C. F. Wang, and S. Chen, *Adv. Sci.* **6**, 1901694 (2019).
- ³⁰X. Wu, Y. Xu, Y. Hu, G. Wu, H. Cheng, Q. Yu, K. Zhang, W. Chen, and S. Chen, *Nat. Commun.* **9**, 4573 (2018).
- ³¹A. J. Brown, N. A. Brunelli, K. Eum, F. Rashidi, J. R. Johnson, W. J. Koros, C. W. Jones, and S. Nair, *Science* **345**(80), 72, (2014).
- ³²C. Hu, H. Sun, Z. Liu, Y. Chen, Y. Chen, H. Wu, and K. Ren, *Biomicrofluidics* **10**, 044112 (2016).
- ³³H. He, C. Yang, F. Wang, Z. Wei, J. Shen, D. Chen, C. Fan, H. Zhang, and K. Liu, *Angew. Chem., Int. Ed.* **59**, 4344 (2020).
- ³⁴Z. Wu, Y. Zheng, L. Lin, S. Mao, Z. Li, and J. M. Lin, *Angew. Chem.* **132**, 2245 (2020).
- ³⁵T. Cubaud and T. G. Mason, *Phys. Rev. Lett.* **96**, 1 (2006).

- ³⁶Y. Yu, F. Fu, L. Shang, Y. Cheng, Z. Gu, and Y. Zhao, *Adv. Mater.* **29**, 1605765 (2017).
- ³⁷P. Xu, R. Xie, Y. Liu, G. Luo, M. Ding, and Q. Liang, *Adv. Mater.* **29**, 1701664 (2017).
- ³⁸H. Ahmed, L. Lee, C. Darmanin, and L. Y. Yeo, *Adv. Mater.* **30**, 1602040 (2018).
- ³⁹M. Steinacher, H. Du, D. Gilbert, and E. Amstad, *Adv. Mater. Technol.* **4**, 1800665 (2019).
- ⁴⁰H. Ahmed, X. Yang, Y. Ehrnst, N. N. Joorje, S. Marqu, P. C. Sherrell, A. El Ghazaly, J. Rosen, A. R. Rezk, and L. Y. Yeo, *Nanoscale Horiz.* **5**, 1050 (2020).
- ⁴¹C. Hu, Y. Bai, M. Hou, Y. Wang, L. Wang, X. Cao, C. W. Chan, H. Sun, W. Li, J. Ge, and K. Ren, *Sci. Adv.* **6**, 1 (2020).
- ⁴²Y. Roig, S. Marre, T. Cardinal, and C. Aymonier, *Angew. Chem., Int. Ed.* **50**, 12071 (2011).
- ⁴³M. Hadjidemetriou and K. Kostarelos, *Nat. Nanotechnol.* **12**, 288 (2017).
- ⁴⁴L. Digiaco, S. Palchetti, F. Giulimondi, D. Pozzi, R. Zenezini Chiozzi, A. L. Capriotti, A. Laganà, and G. Caracciolo, *Lab Chip* **19**, 2557 (2019).
- ⁴⁵A. C. G. Weiss, K. Krüger, Q. A. Besford, M. Schlenk, K. Kempe, S. Förster, and F. Caruso, *ACS Appl. Mater. Interfaces* **11**, 2459 (2019).
- ⁴⁶I. Srivastava, M. S. Khan, K. Dighe, M. Alafeef, Z. Wang, T. Banerjee, T. Ghonge, L. M. Grove, R. Bashir, and D. Pan, *Small Methods* **4**, 2000099 (2020).
- ⁴⁷H. Cheng, S. Tang, T. Yang, S. Xu, and X. Yan, *Angew. Chem., Int. Ed.* **59**, 19862 (2020).
- ⁴⁸Z. Wei, Y. Li, R. G. Cooks, and X. Yan, *Annu. Rev. Phys. Chem.* **71**, 31 (2020).
- ⁴⁹M. Faustini, J. Kim, G. Y. Jeong, J. Y. Kim, H. R. Moon, W. S. Ahn, and D. P. Kim, *J. Am. Chem. Soc.* **135**, 14619 (2013).
- ⁵⁰X. Zhong, H. Chen, and R. N. Zare, *QRB Discovery* **2**, 0 (2021).
- ⁵¹J. K. Lee, K. L. Walker, H. S. Han, J. Kang, F. B. Prinz, R. M. Waymouth, H. G. Nam, and R. N. Zare, *Proc. Natl. Acad. Sci. U.S.A.* **116**, 19294 (2019).
- ⁵²J. K. Lee, H. S. Han, S. Chaikasetin, D. P. Marron, R. M. Waymouth, F. B. Prinz, and R. N. Zare, *Proc. Natl. Acad. Sci. U.S.A.* **117**, 30934 (2020).
- ⁵³J. M. Campos-Martin, G. Blanco-Brieva, and J. L. G. Fierro, *Angew. Chem., Int. Ed.* **45**, 6962 (2006).
- ⁵⁴H. Xiong, J. K. Lee, R. N. Zare, and W. Min, *J. Phys. Chem. Lett.* **11**, 7423 (2020).
- ⁵⁵C. F. Chamberlayne and R. N. Zare, *J. Chem. Phys.* **152**, 184702 (2020).
- ⁵⁶Y. Zhu, Z. Huang, Q. Chen, Q. Wu, X. Huang, P. K. So, L. Shao, Z. Yao, Y. Jia, Z. Li, W. Yu, Y. Yang, A. Jian, S. Sang, W. Zhang, and X. Zhang, *Nat. Commun.* **10**, 4049 (2019).
- ⁵⁷S. M. Kang, B. Park, G. S. R. Raju, S. Baek, S. K. Hussain, C. H. Kwak, Y. K. Han, J. S. Yu, S. W. Kim, and Y. S. Huh, *Chem. Eng. J.* **384**, 123316 (2020).
- ⁵⁸H. Song, D. L. Chen, and R. F. Ismagilov, *Angew. Chem., Int. Ed.* **45**, 7336 (2006).
- ⁵⁹I. Lignos, S. Stavrakis, G. Nedelcu, L. Protesescu, A. J. Demello, and M. V. Kovalenko, *Nano Lett.* **16**, 1869 (2016).
- ⁶⁰M. J. Jebrail, A. H. C. Ng, V. Rai, R. Hili, A. K. Yudin, and A. R. Wheeler, *Angew. Chem.* **122**, 8807 (2010).
- ⁶¹D. Witters, N. Vergauwe, R. Ameloot, S. Vermeir, D. De Vos, R. Puers, B. Sels, and J. Lammertyn, *Adv. Mater.* **24**, 1316–1320 (2012).
- ⁶²H. Sun, W. Li, Z. Z. Dong, C. Hu, C. H. Leung, D. L. Ma, and K. Ren, *Biosens. Bioelectron.* **99**, 361 (2018).
- ⁶³H. Song, J. D. Tice, and R. F. Ismagilov, *Angew. Chem.* **115**, 792 (2003).
- ⁶⁴I. Shestopalov, J. D. Tice, and R. F. Ismagilov, *Lab Chip* **4**, 316 (2004).
- ⁶⁵M. Chabert, K. D. Dorfman, and J. L. Viovy, *Electrophoresis* **26**, 3706 (2005).
- ⁶⁶A. R. Abate, T. Hung, P. Marya, J. J. Agresti, and D. A. Weitz, *Proc. Natl. Acad. Sci. U.S.A.* **107**, 19163 (2010).
- ⁶⁷T. Gu, C. Zheng, F. He, Y. Zhang, S. A. Khan, and T. A. Hatton, *Lab Chip* **18**, 1330 (2018).
- ⁶⁸K. Ren, J. Zhou, and H. Wu, *Acc. Chem. Res.* **46**, 2396 (2013).
- ⁶⁹K. Ren, W. Dai, J. Zhou, J. Su, and H. Wu, *Proc. Natl. Acad. Sci. U.S.A.* **108**, 8162 (2011).
- ⁷⁰H. Sun, C. W. Chan, Y. Wang, X. Yao, X. Mu, X. Lu, J. Zhou, Z. Cai, and K. Ren, *Lab Chip* **19**, 2915 (2019).
- ⁷¹Y. Wang, S. Chen, H. Sun, W. Li, C. Hu, and K. Ren, *Microphysiological Syst.* **2**, 6 (2018).

30 October 2023 05:49:19